Deciphering the Binding Behaviours of BSA Using Ionic AIE-active Fluorescent Probes

Jiaqi Tong,[a] Ting Hu,[a] Anjun Qin,[c] Jing Zhi Sun,*[a] Ben Zhong Tang*[abc]

[a] *MoE Key Laboratory of Macromolecular Synthesis and Functionalization, Department of Polymer Science and Engineering, Zhejiang University, Hangzhou 310027, China. Email: sunjz@zju.edu.cn.*

[b] *Department of Chemistry, Division of Biomedical Engineering, Hong Kong Branch of Chinese National Engineering Research Center for Tissue Restoration and Reconstruction, Institute for Advanced Study, Division of Life Science, Institute of Molecular Functional Materials and State Key Laboratory of Molecular Neuroscience, The Hong Kong University of Science & Technology (HKUST). Email: tangbenz@ust.hk.*

[c] *Guangdong Innovative Research Team, State Key Laboratory of Luminescent Materials and Devices, South China University of Technology, Guangzhou 510640, China.*

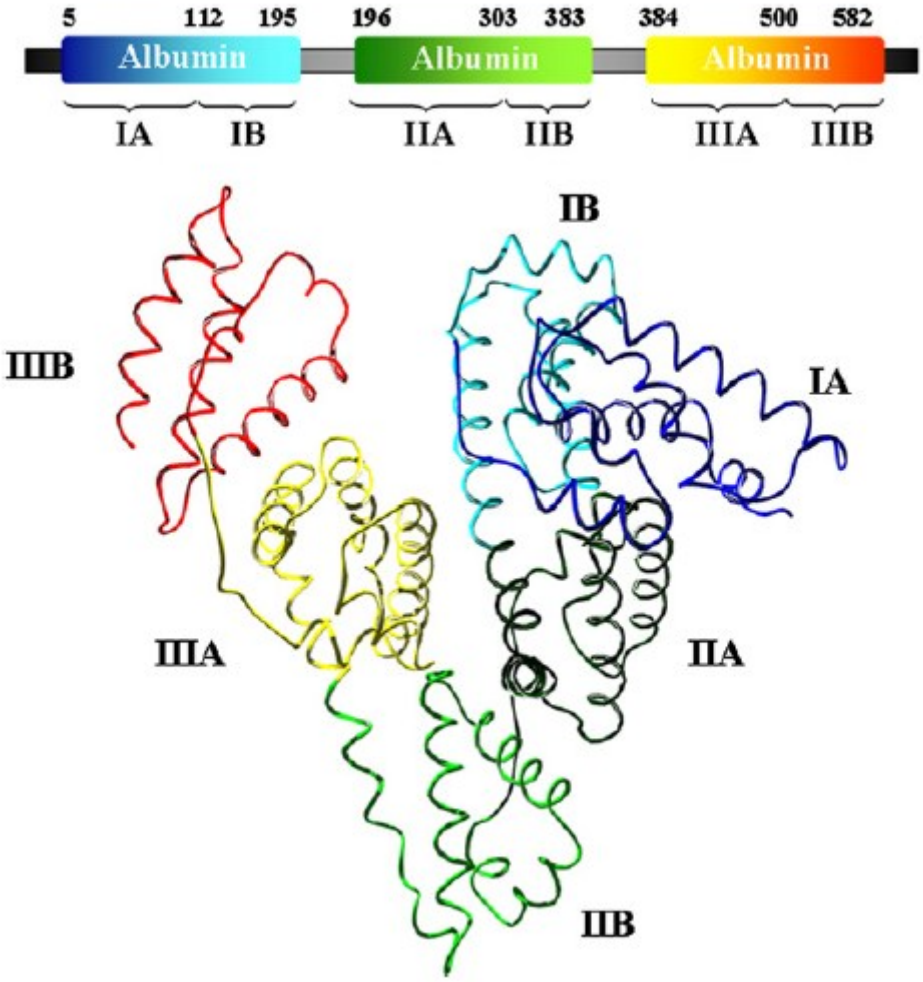

Figure S1. Conformational structure of BSA in its native state.

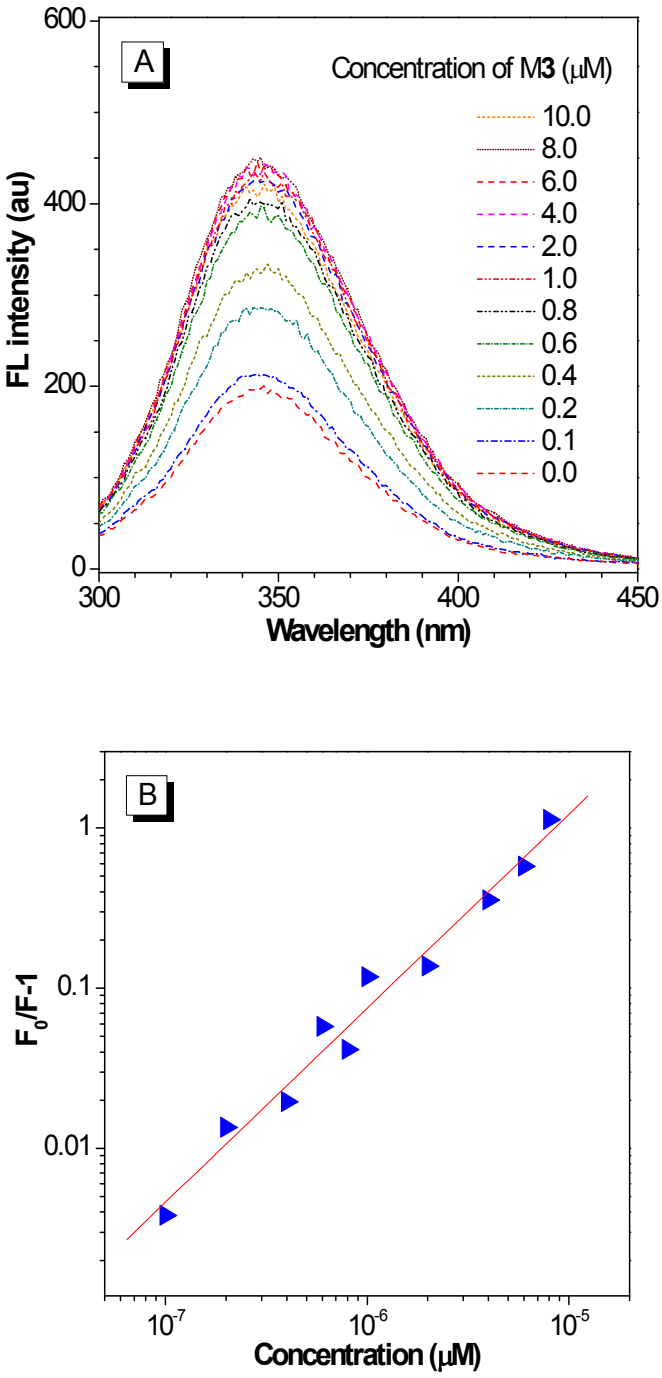

Figure S2. (A) FL spectra of BSA (1 μM) excited at 280 nm in the presence of different concentrations of M**3**; (B) Plot of lg [(F_0-F)/F] *vs.* lg [M**3**]. F_0 and F: the peak FL intensity of BSA without the probe and with different concentrations of the probe.

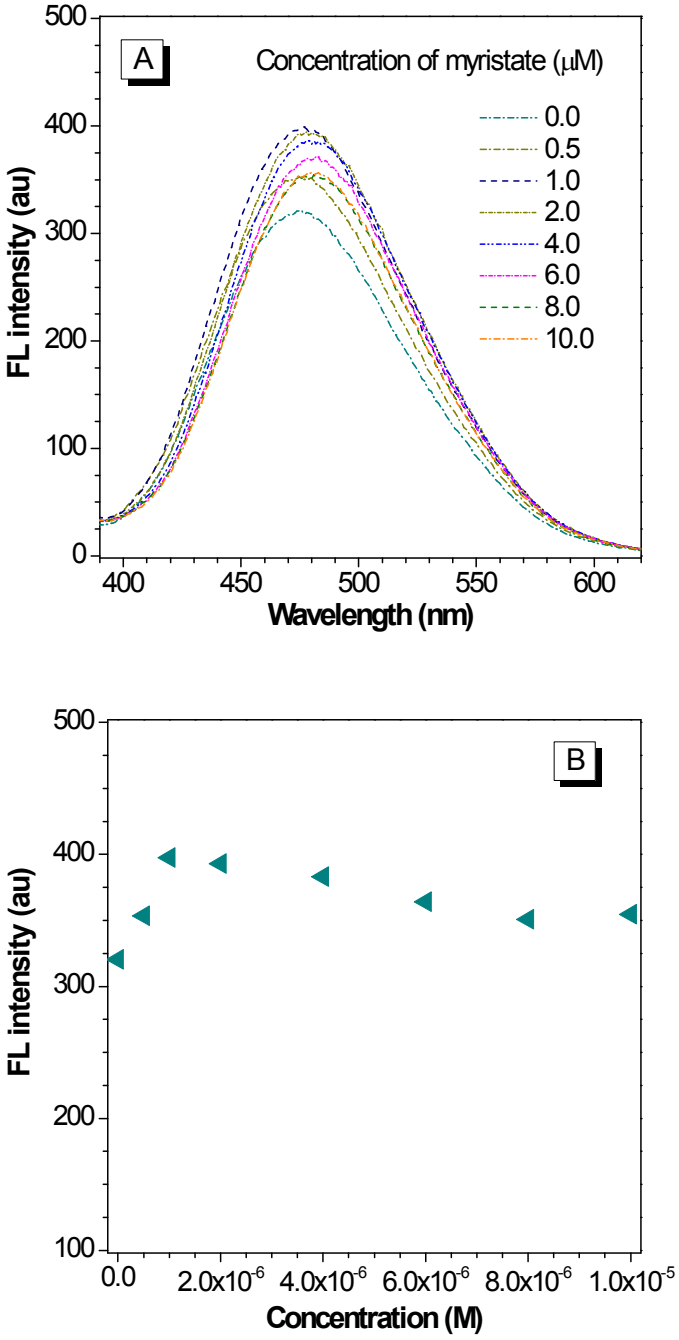

Figure S3. (A) FL spectra of BSA+M**2** system in the presence of different concentrations of myristic acid (0~10 μM). (B) Plots of the corresponding fluorescent intensities. Excitation wavelength (λ_{ex}) : 330 nm. Concentration of M**2**: 1 μM; Concentration of BSA: 1 μM.

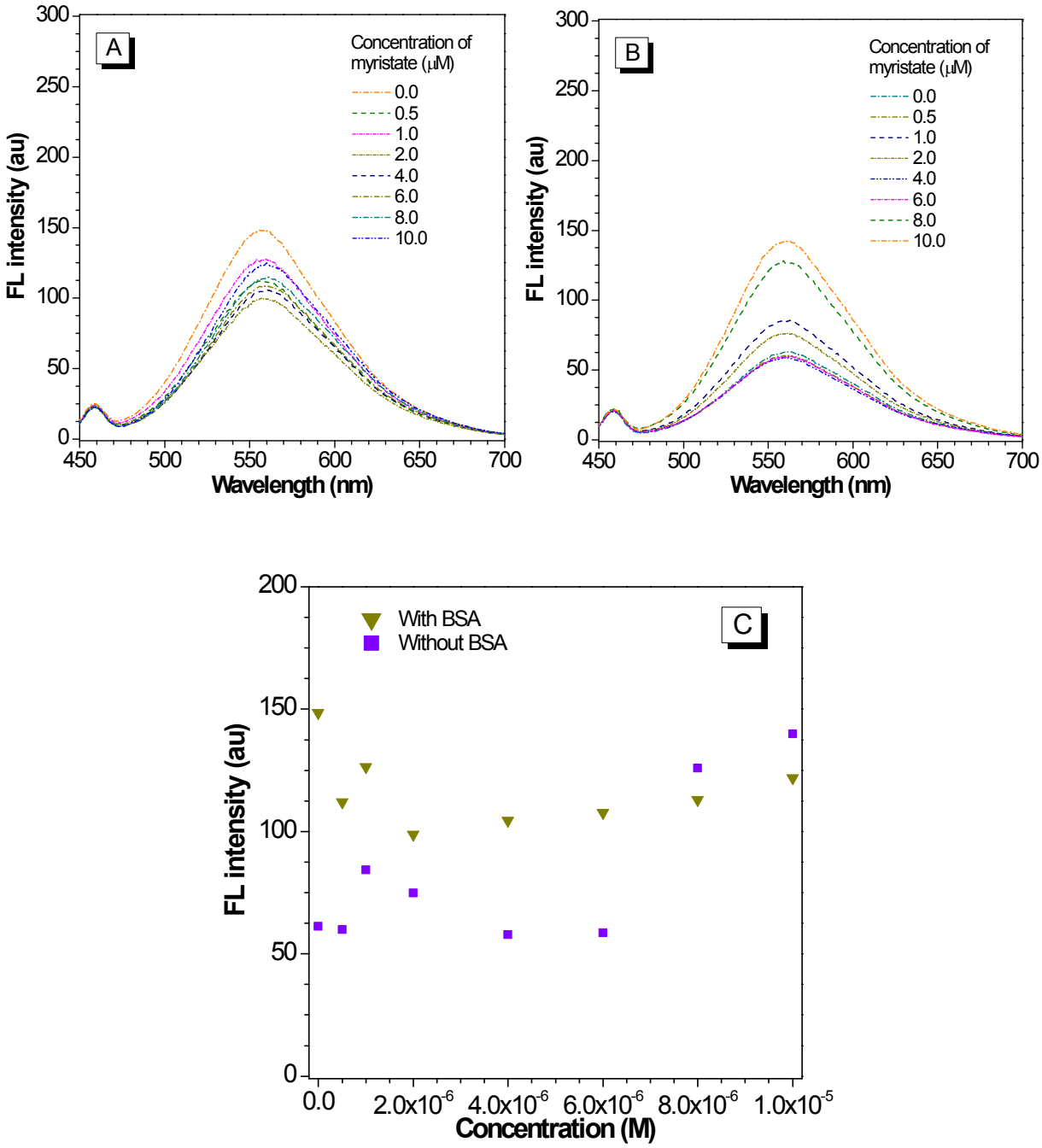

Figure S4. (A) FL spectra of BSA+M**3** with different concentrations (0~10 μM) of myristic acid; (B) FL spectra of M**3** with different concentrations (0~10 μM) of myristic acid; (C) Plots of the corresponding fluorescent intensities. λ_{ex}: 395 nm. Concentration of M**3**: 1 μM; Concentration of BSA: 1 μM.

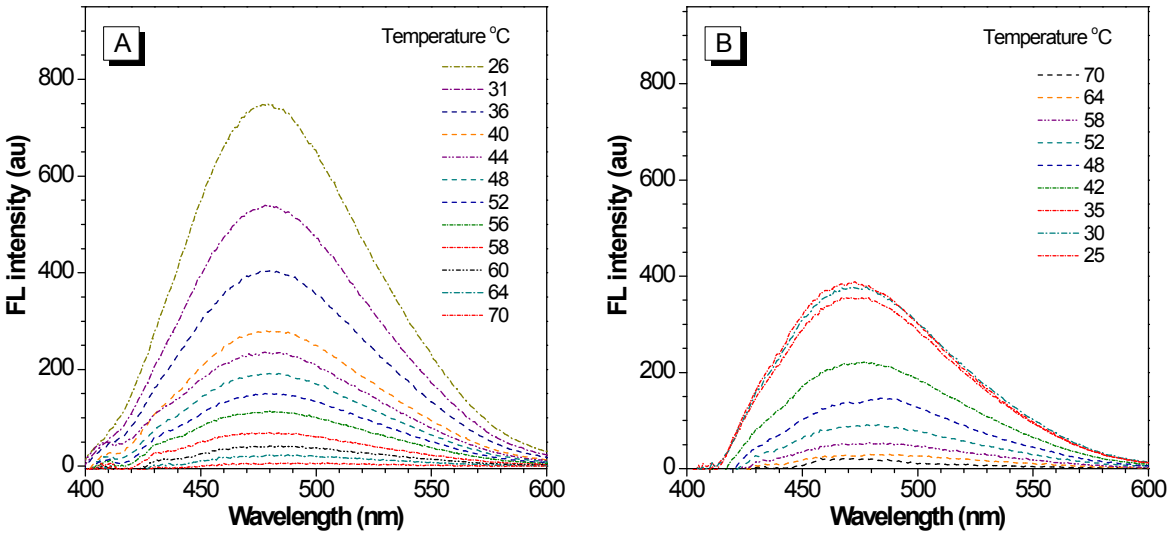

Figure S5. FL spectra of BSA+M**2** system in PBS buffer (pH=7.4) at different temperatures (heating from 25 °C to 75 °C, and then cooling from 75 °C to 25 °C). λ_{ex}: 330 nm. Concentration of M**2**: 5 μM; Concentration of BSA: 1 μM.

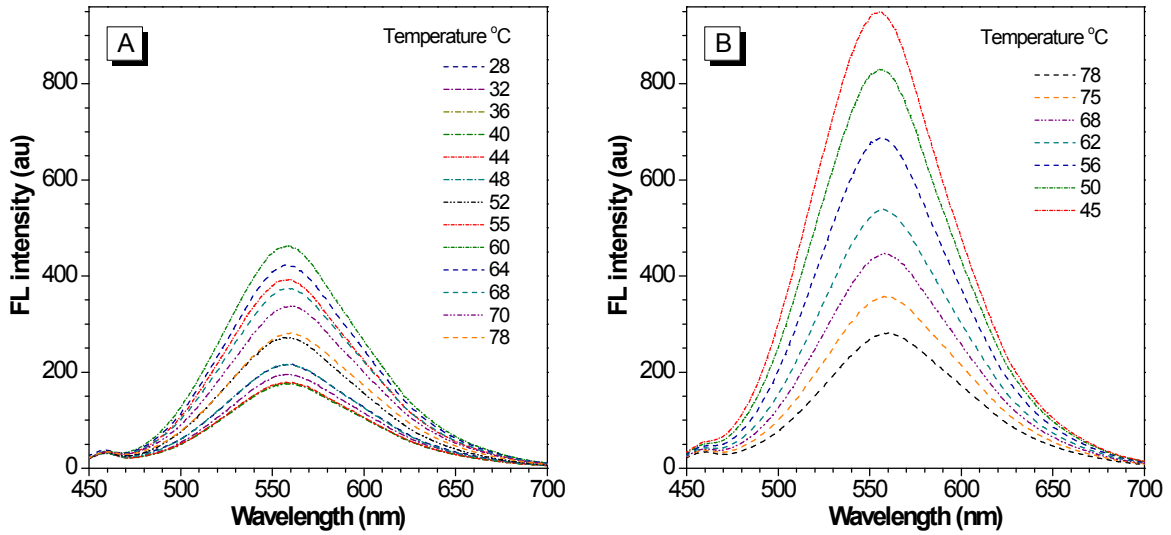

Figure S6. FL spectra of BSA+M**3** system in PBS buffer (pH=7.4) at different temperatures (heating from 25 °C to 75 °C, and then cooling from 75 °C to 25 °C). λ_{ex}: 395 nm. Concentration of M**3**: 5 μM; Concentration of BSA: 1 μM.

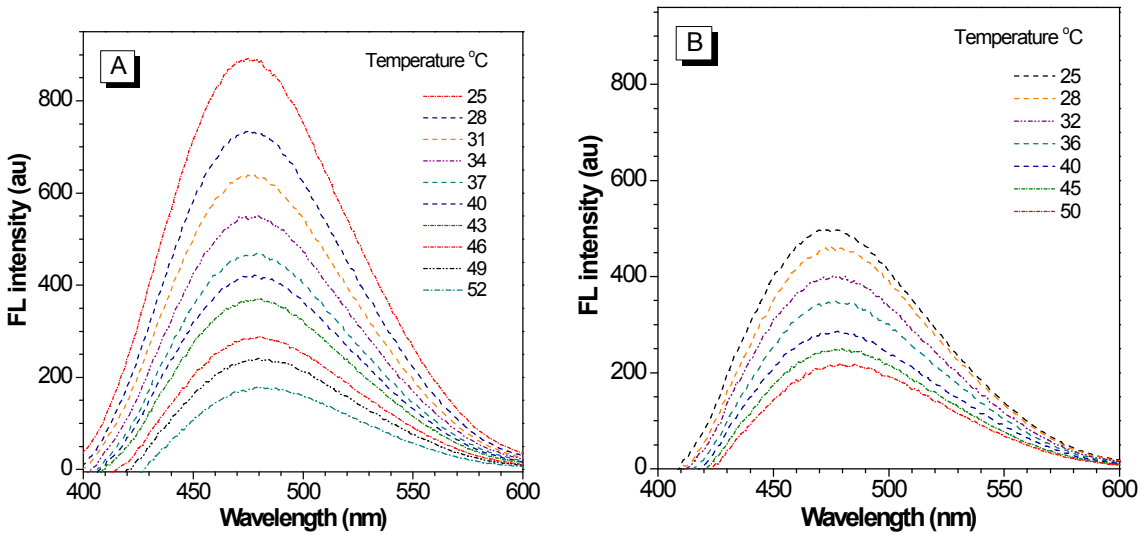

Figure S7. FL spectra of BSA+M**2** system in PBS buffer (pH=7.4) at different temperatures (heating from 25 °C to 50 °C and then cooling from 50 °C to 25 °C). λ_{ex}: 330 nm. Concentration of M**2**: 5 μM; Concentration of BSA: 1 μM.

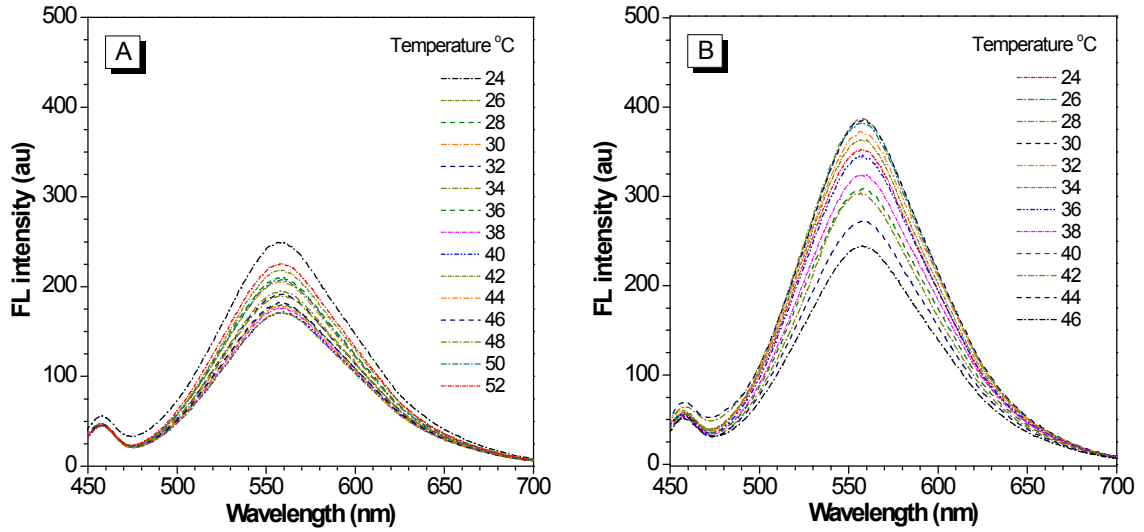

Figure S8. FL spectra of BSA+M**3** system in PBS buffer (pH=7.4) at different temperatures (heating from 25 °C to 50 °C, and then cooling from 50 °C to 25 °C). λ_{ex}: 395 nm. Concentration of M**3**: 5 μM; Concentration of BSA: 1 μM.

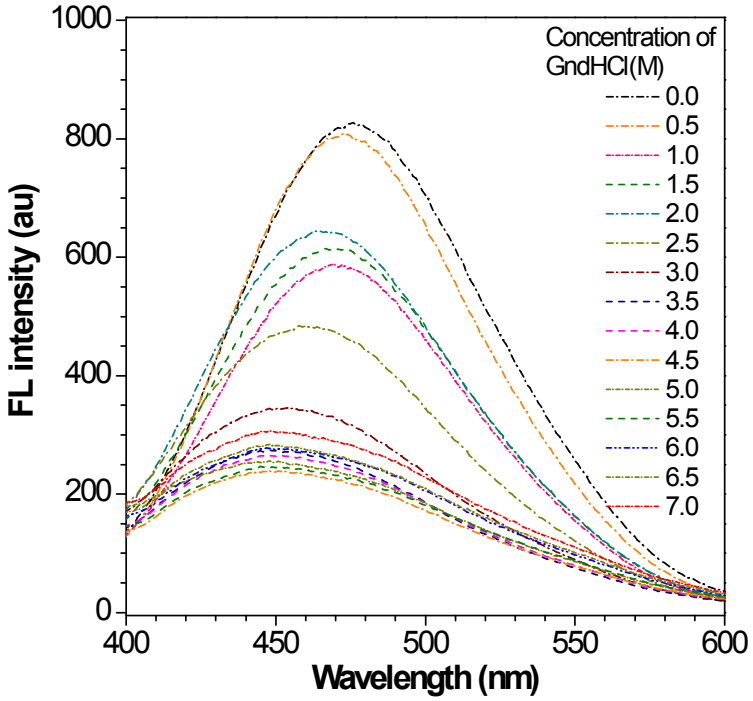

Figure S9. FL spectra of BSA+M**2** system in the presence of different concentrations of GndHCl. λ_{ex}: 330 nm; Concentration of M**2**: 1 μM; Concentration of BSA: 1 μM.

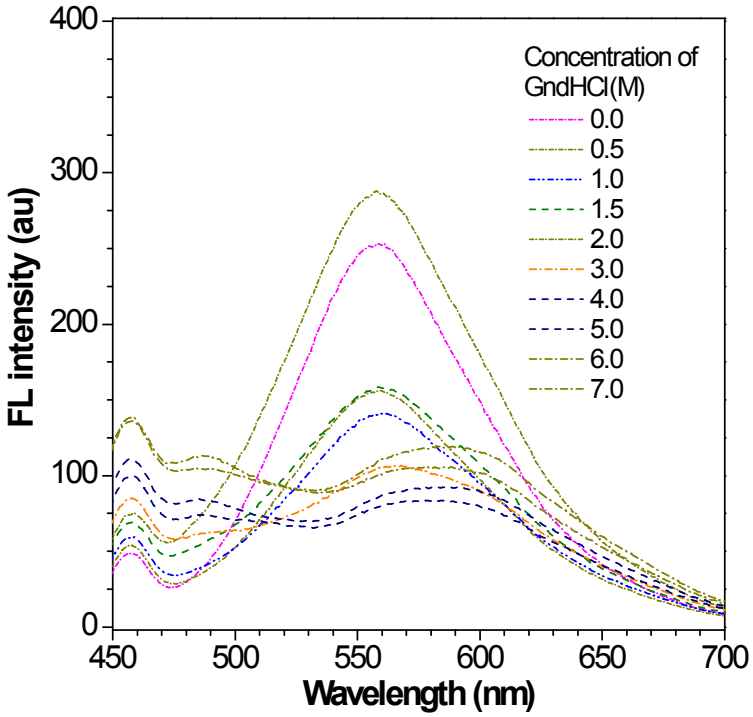

Figure S10. FL spectra of BSA+M**3** system in the presence of different concentrations of GndHCl. λ_{ex}: 395 nm; Concentration of M**3**: 1 μM; Concentration of BSA: 1 μM.

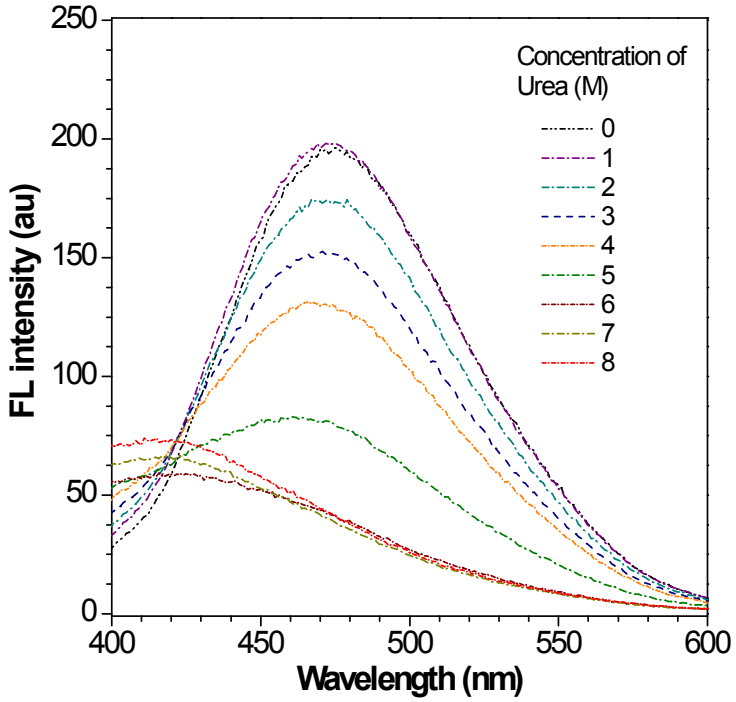

Figure S11. FL spectra of BSA+M**2** system in the presence of different concentrations of urea. λ_{ex}: 330 nm; Concentration of M**2**: 1 μM; Concentration of BSA: 1 μM.

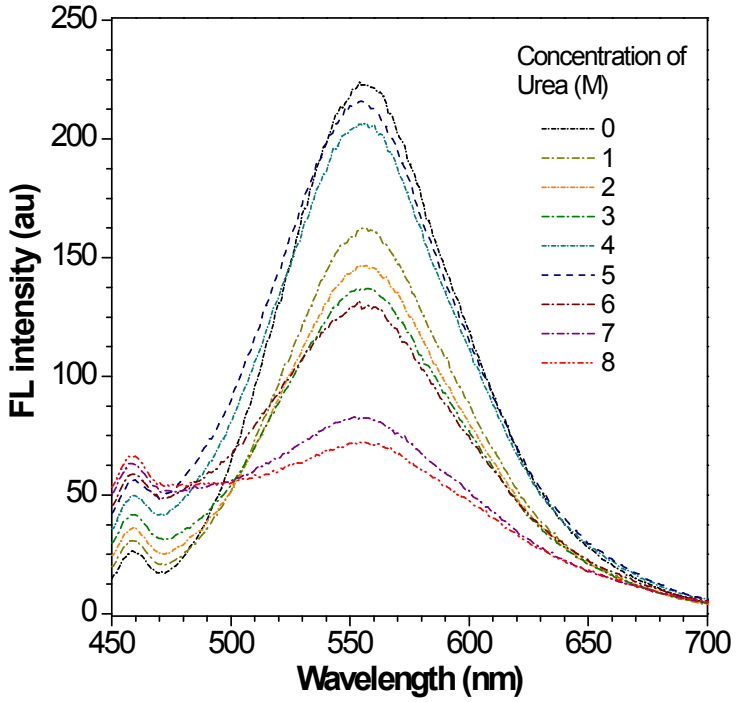

Figure S12. FL spectra of BSA+M**3** system in the presence of different concentrations of urea. λ_{ex}: 395 nm; Concentration of M**3**: 1 μM; Concentration of BSA: 1 μM.

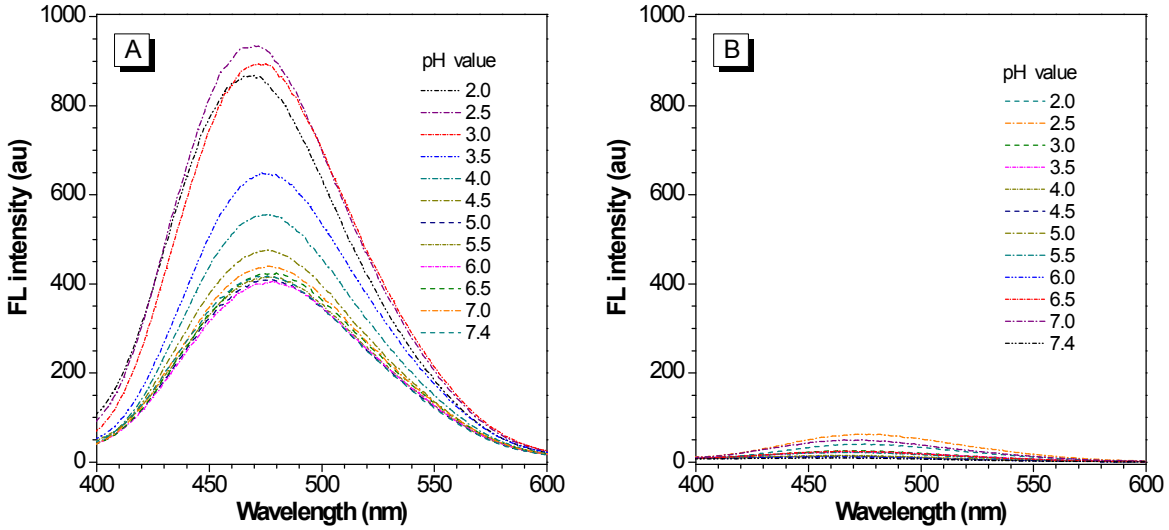

Figure S13. FL spectra of M**2** in the presence (A) or absence (B) of BSA in buffer with different pH values (2.0~7.4). λ_{ex}: 330 nm; Concentration of M**2**: 1 μM; Concentration of BSA: 1 μM.

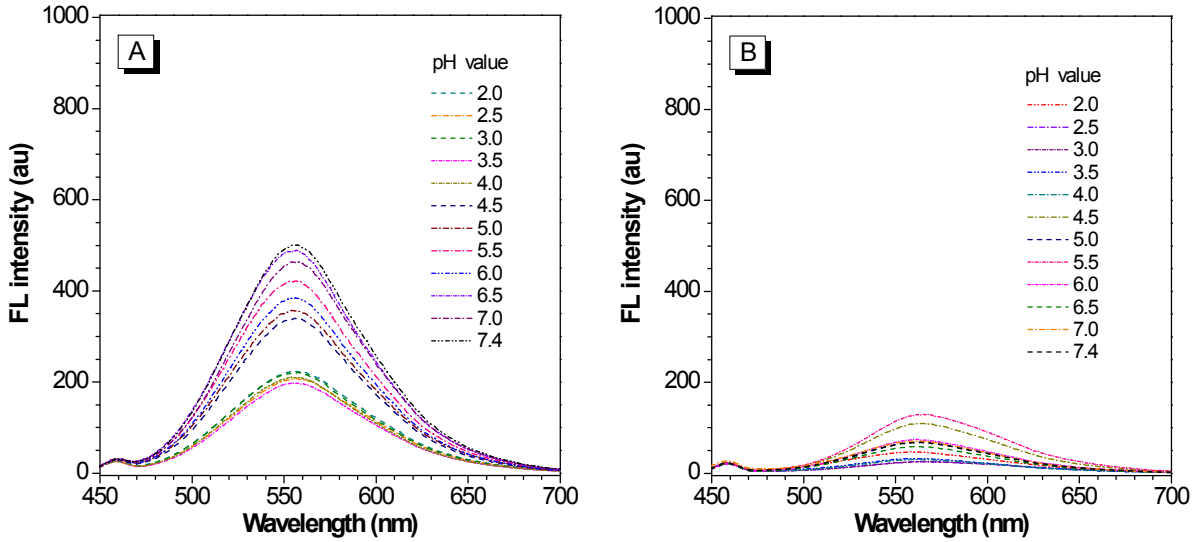

Figure S14. FL spectra of M**3** in the presence (A) or absence (B) of BSA in buffer with different pH values (2.0~7.4). λ_{ex}: 395 nm; Concentration of M**3**: 1 μM; Concentration of BSA: 1 μM.